Current Biology, Volume *29*

Supplemental Information

Visually Guided Behavior and Optogenetically Induced Learning in Head-Fixed Flies Exploring a Virtual Landscape

Hannah Haberkern, Melanie A. Basnak, Biafra Ahanonu, David Schauder, Jeremy D. Cohen, Mark Bolstad, Christopher Bruns, and Vivek Jayaraman

Virtual reality setup

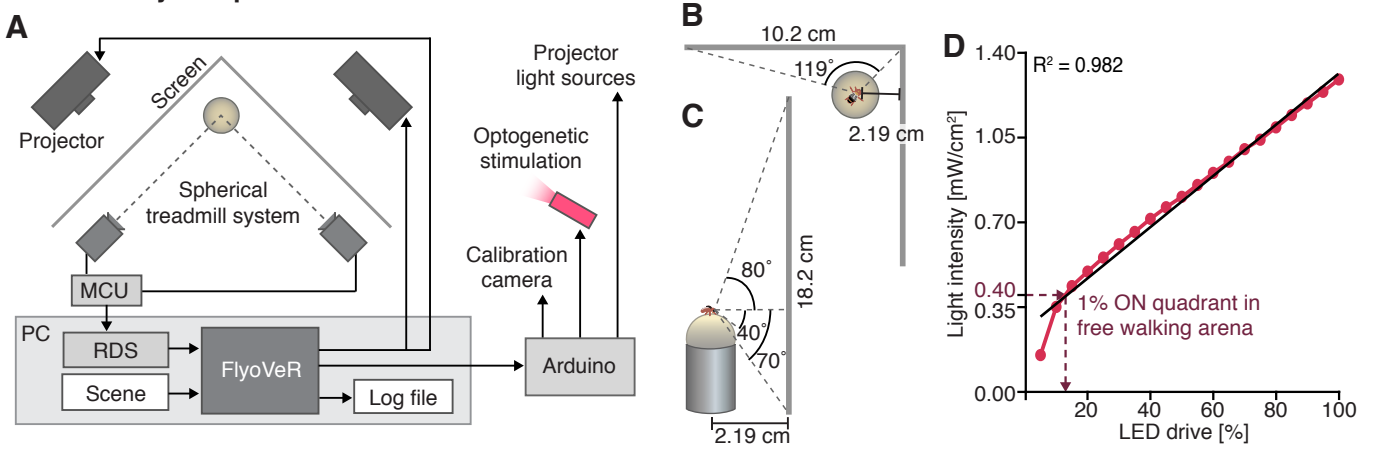

Virtual world design

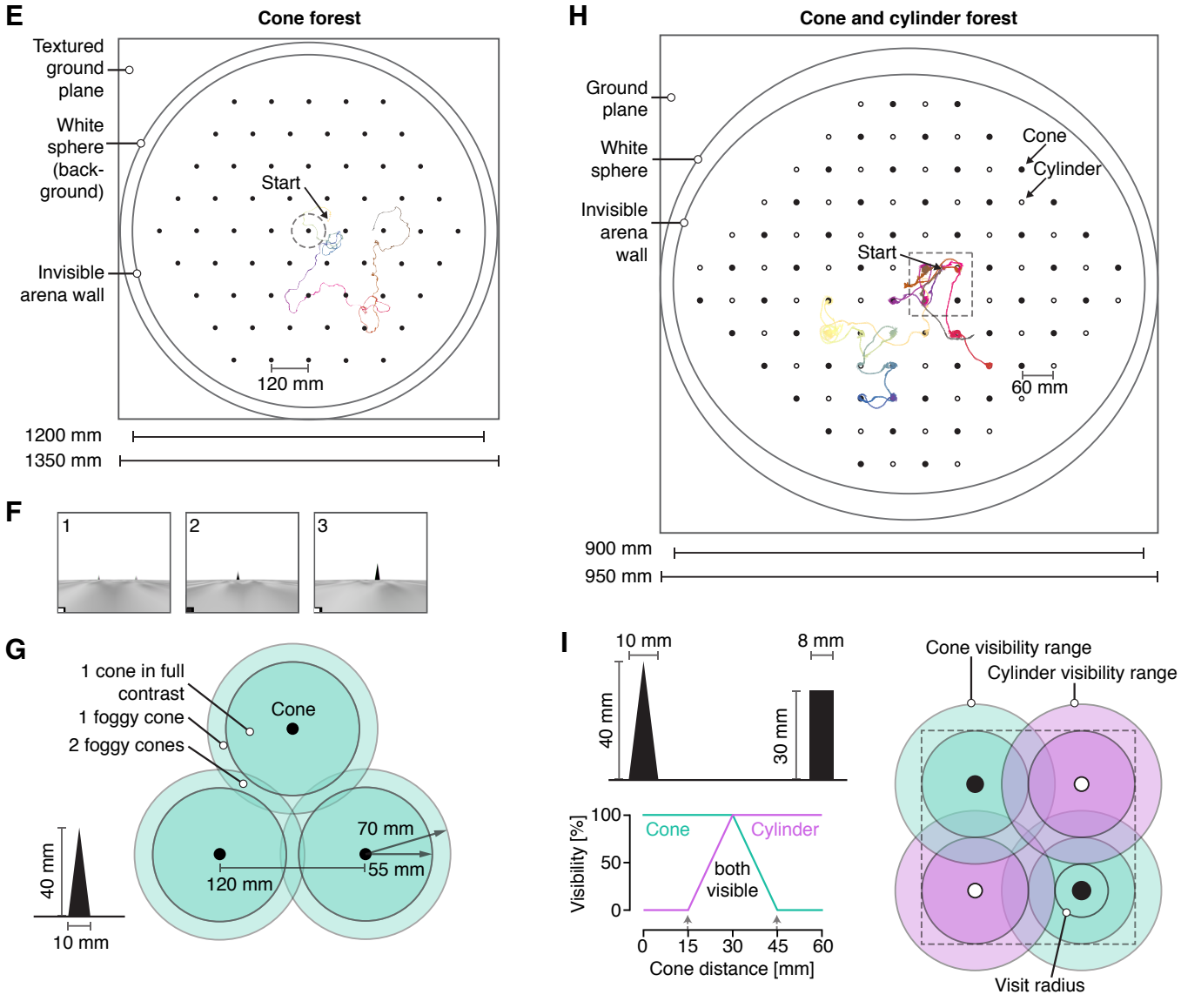

Figure S1: Design of the 2D VR system, Related to Figure 1.
(**A**-**D**) Extended information on the hardware and software of the VR system. (**A**) Schematic of the hardware and software control loops. RDS, remote data server; MCU, microcontroller unit. (**B, C**) Schematic illustrating the size of the visual display screen and its position relative to the fly on the treadmill. View from the side (C) and top (B). The range of the horizontal field of view indicated in (C) corresponds to the closest screen distance relative to the fly, which occurs at 90˚ on both sides. The virtual scene horizon is positioned at the height of the ball (dashed horizontal line) (**D**) Light intensity measured on the ball surface with a power meter (Methods) for different input LED drives. Overall the relationship between LED drive and light intensity was well described by a linear fit ($y = 0.05 x + 0.26$, $R^2 = 0.98$). (**E-I**) Design of the periodic virtual worlds. (**E**) Schematic of the complete *cone forest* scene with an example trajectory from a 10 min trial overlaid. (**F**) Screenshots taken at different time points during the approach of a virtual cone. They reflect the distortion that was used to account for the screen geometry. (**G**) In the periodic world design, virtual objects (cones) are positioned on the nodes of equilateral triangles that form the unit cell of a large hexagonal grid. The shortest distance between two adjacent cones is 120 mm. The two shaded circles around each cone indicate the where the respective cone begins to be visible (lightly shaded circle: 70 mm radial distance) and where it starts to appear in full contrast (darker shaded circle: 55 mm radial distance). Cones were 10 mm wide at the base and 40 mm tall. (**H**) Schematic of the *cone and cylinder forest* scene with an example trajectory from a male HC-Gal4 > ChrimsonR fly (10 min pre-trial, group trained against the cylinder; Methods). The dashed circle in (E) and the square in (H) indicate the “unit cells” onto which walking trajectories through the periodic scene are projected. Note the different spatial scales in the schematics in (E) and (H). (**I**) Schematic illustrating cone and cylinder placement, dimensions and virtual fog settings in the *cone and cylinder forest* scene. Graphic on the right illustrates visibility with shaded circles around each object analogously to (G).

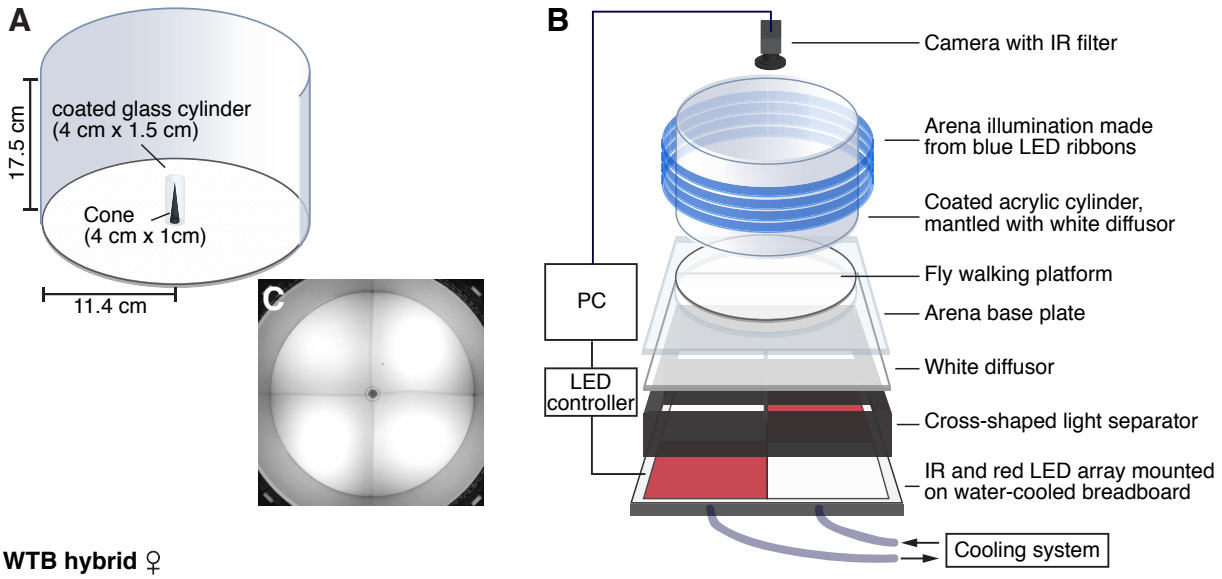

WTB hybrid ♀

Free walking (n=20, 10 min trial)

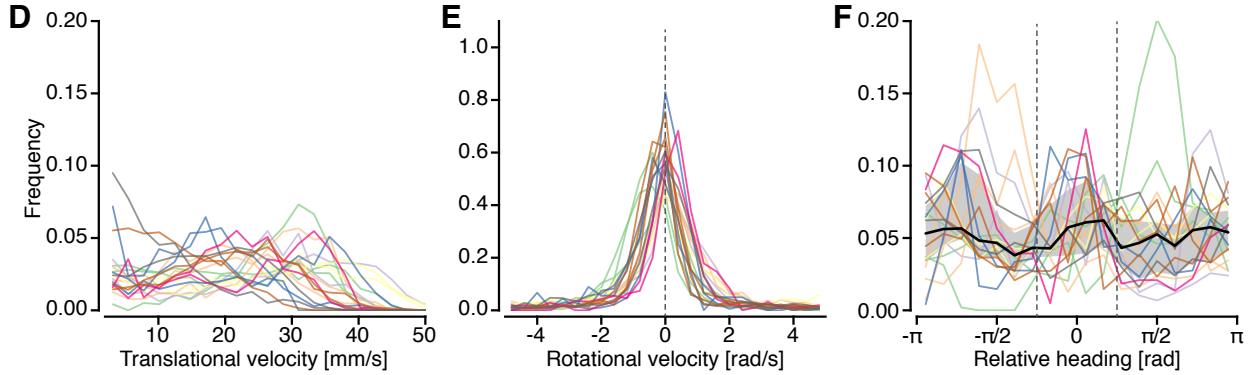

Virtual reality (n=20, first 10 min trial)

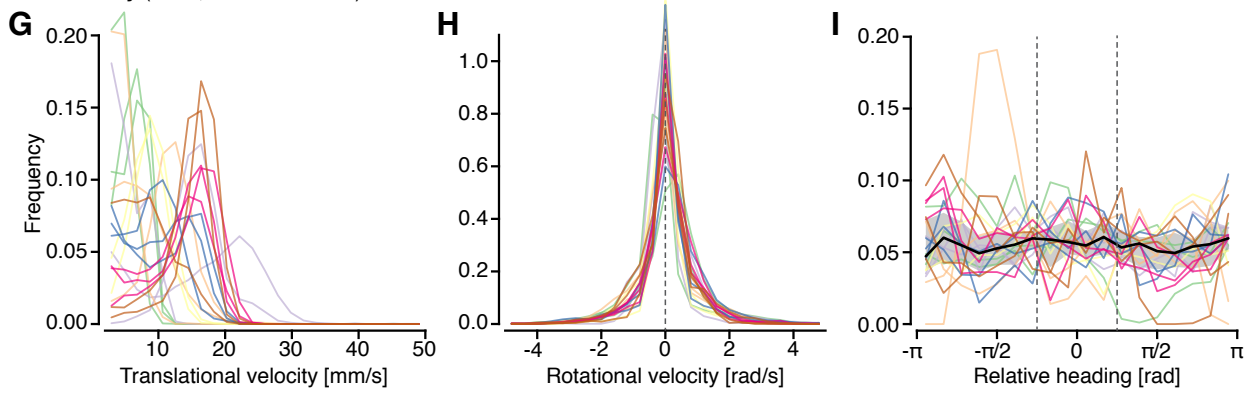

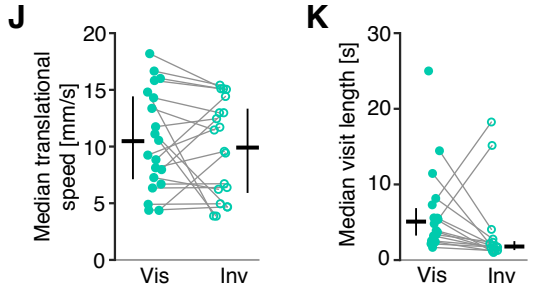

Figure S2: Extended data on object interaction in freely and tethered walking flies, Related to Figure 2.

(**A**) Schematic of the free walking arena with a cone and a glass cylinder that prevents flies from climbing onto the object. (**B**) Schematic of the entire free walking rig. (**C**) Video frame from a trial with a male fly (visible in upper right arena quadrant) exploring the arena with a cone. The image was taken with an IR camera and does not reflect the lighting conditions visible to the fly. (**D**-**I**) Data from female WTB hybrid flies free walking trials (D-F, n = 20) and VR trials (G-I, n = 20, only first out of three VR trials with visible objects included). Fly identity is color-coded. (**D**, **G**) Frequency distribution of the translational velocity. (**E**, **H**) Frequency distribution of the rotational velocity. (**F**, **I**) Relative heading distributions. The black line and grey shaded region indicate median and interquartile range (IQR, between the 25th and 75th quartile). Relative heading angle bin size: 20 ˚. For free walking data, only trajectories within 10 mm – 60 mm radial distance from the object (center of the arena) were considered in the analysis. (**J, K**) Extended data on interaction with visible and invisible virtual objects in VR (female WTB hybrid, n = 20). Visualization as in Figure 2H,I. (**J**) Comparison of median translational speed of walking flies. (**K**) Median visit length (time spent within 15 mm radius around object). WTB hybrid, hybrid generated from WTB and empty-Gal4 line.

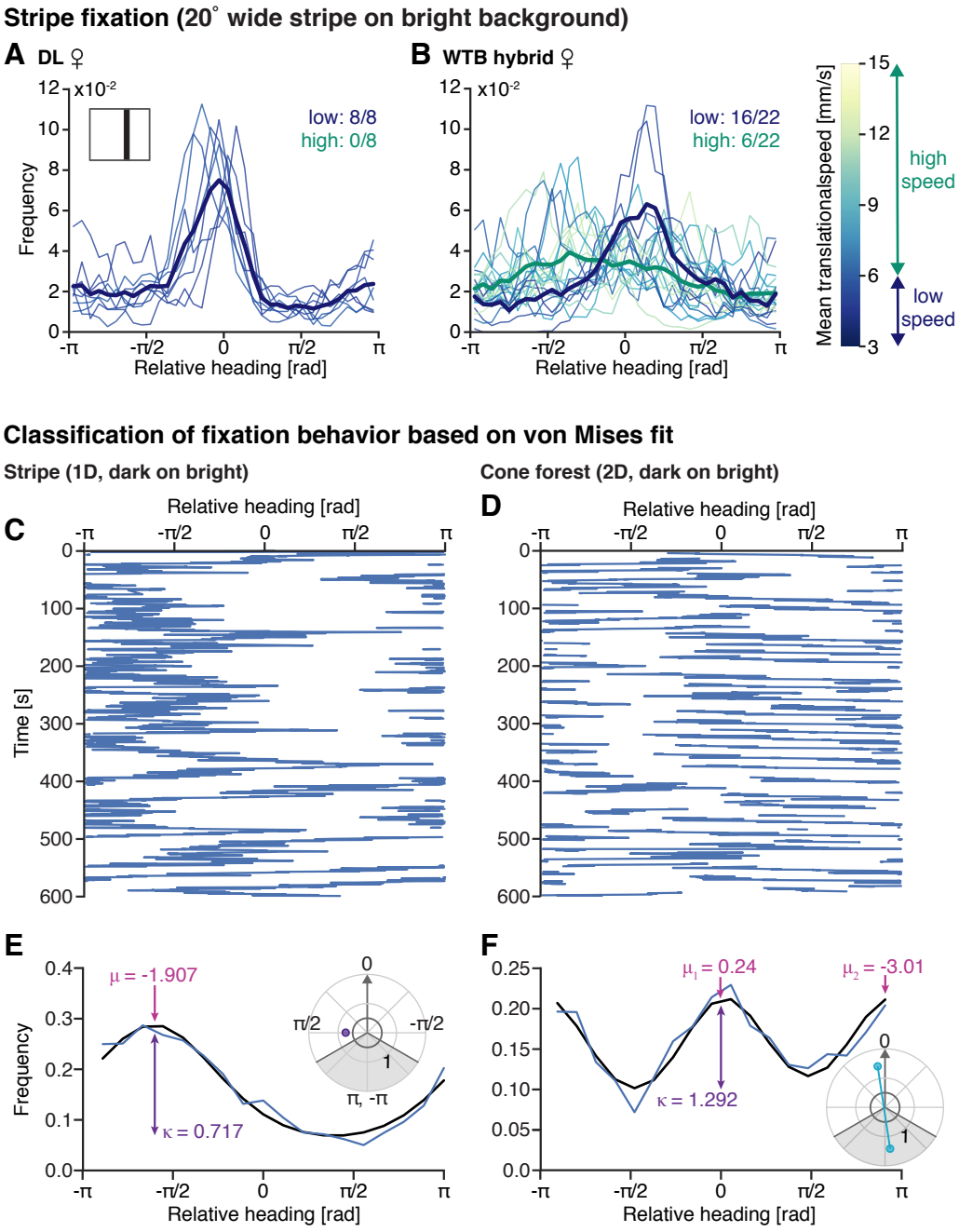

Figure S3: Extended data on stripe and object fixation, Related to Figure 3.
(**A, B**) Stripe fixation behavior was more pronounced in slowly walking flies. Relative heading distributions calculated from data of female DL flies (A, n = 8 selected from 10 flies based on walking activity) and female WTB hybrid flies (B, n = 22 selected from 25 based on walking activity). Median distributions are calculated after separating flies into two groups based on their mean translations speed computed over the full trial (criterion: more or less than 6 mm/s translational speed). Bin size 10 ˚. DL, Dickinson lab strain. In experiments with DL, the wings were glued, while in experiments with WTB hybrid flies, the wings were cut. (**C-F**) Classification of fixation behavior based on von Mises fit. All data from female WTB hybrid flies. (**C, D**) Time series of the relative heading angle of two female WTB flies (cut wings, 30 ˚C room temperature) over a 10 min trial with either a dark 20 ˚ wide stripe on bright background (C) or in a dark 2D plane with bright objects (D). (**E, F**) Blue line: Relative heading distributions computed from the time series shown in (C, D), respectively. Black line: von Mises fit to the measured distribution. In (E) a unimodal and in (F) a bimodal von Mises distribution was fitted. The location (μ) and shape (κ) parameters are indicated in the plot. See Methods for details on the fitting procedure.

Local search in groups of freely walking flies

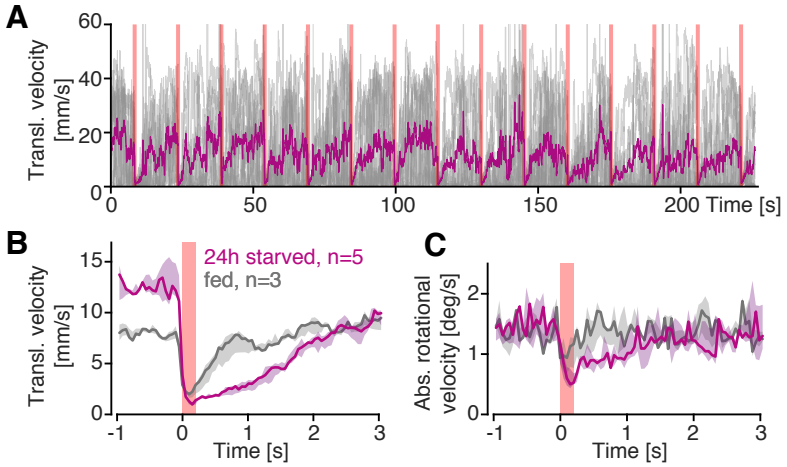

Local search in VR

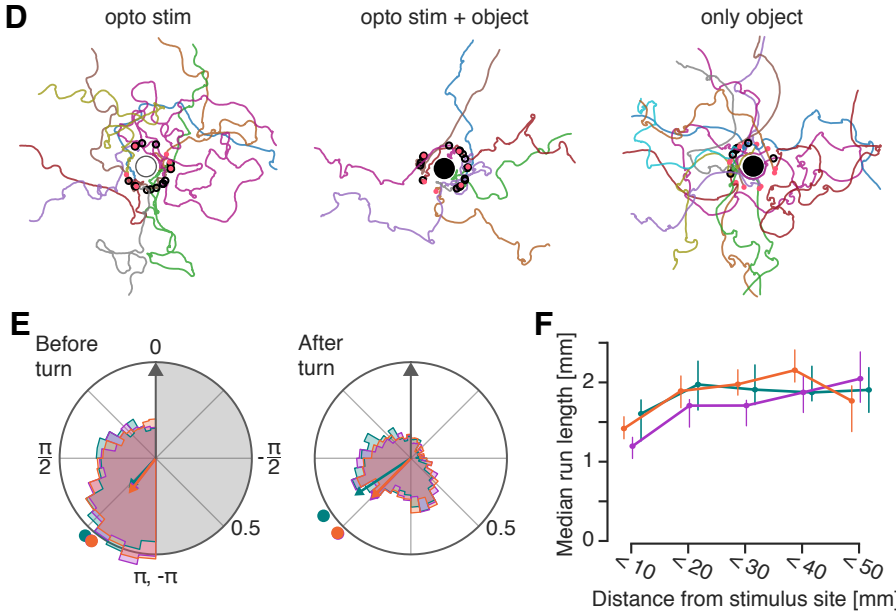

1s long optogenetic stimulation

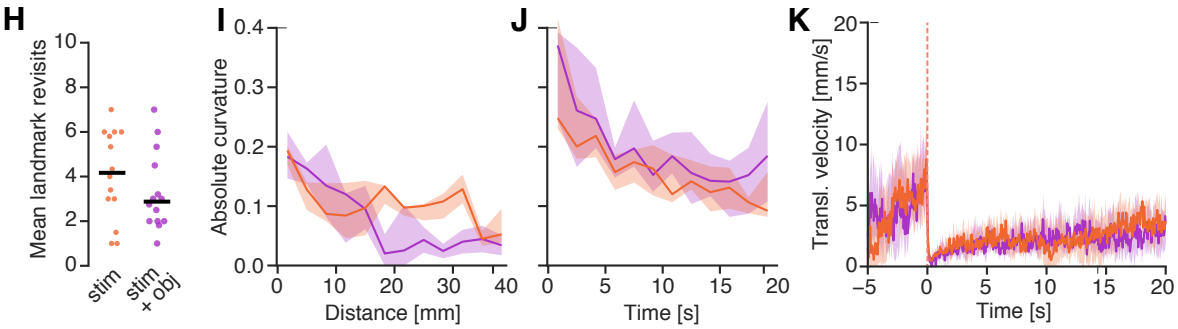

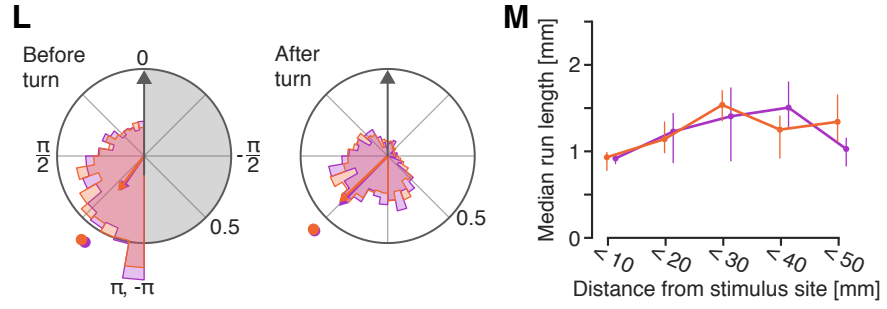

Figure S4: Extended data on optogenetically induced local search, Related to Figure 4.
(**A**-**C**) Effect of optogenetic activation of sugar sensing neurons on walking velocity in freely moving flies. (**A**) Translational walking velocity of female Gr64f > ChrimsonR flies (24 h starved) over the time course of a protocol consisting of 15 light stimulation pulses (200 ms, 1.58 mW/cm^2) each separated by a 15 s break. Walking behavior was measured in groups of ~10 flies. Grey lines: velocity traces from individual flies. Purple line: Mean translational velocity across flies. (**B**, **C**) Average response of 24 h starved (purple) and fed (grey) flies to a stimulation pulse. The responses in translational (B) and rotational (C) walking velocity are shown as averages (median and interquartile range) across experimental repeats (starved group: n = 5, fed group: n=3). For each repeat, responses were averaged (mean) across flies and subsequently across the 15 stimulus repetitions. (**D**) Illustration of all local search bouts (see Methods for details) of a single fly for the three experimental groups presented in Figure 4. Each search bout is plotted in a different color. Small salmon dots indicate optogenetic stimulation events and small black empty circles indicate successive visits (10 mm radius). Invisible or visible cone location is marked by an empty or filled circle, respectively. (**E, F**) Analysis of walking behavior during search bouts. (**E**) Polar histogram of heading angles relative to the cone (or center of the reward site) immediately before (left) and after (right) a large turn (>π/8 radians change in heading). Angles were mirrored such that all turns started with the stimulation site on the right. Arrows show the population vector average for each group, and dots mark the location of the circular mean. Minimal object distance 6 mm. Number of large turns (total number of turns): 2,660 (5,507) for “opto stim”, 2,136 (4,837) for “opto stim + object”, 1,465 (3,810) for “only object”. (**F**) Median run length as a function of radial distance from the cone (or center of the reward site). Vertical lines indicate 95% confidence intervals determined through bootstrapping. Minimum run length: 0.5 mm. Minimal object distance 6 mm. Number of runs: 2,944 for “opto stim”, 2,534 for “opto stim + obj”, 1,934 for “only obj”. (**G**) Sampling of different virtual food patches over the course of the full 20 min trial, as measured by the total number of different landmarks visited by individual flies. (**H-M**) Same quantification of walking behavior as in Figure 4F-I (for panels H-K) and S5D,C (for panels L,M), but for a dataset with 1 s long optogenetic stimulation events. For (L), the number of large turns (total number of turns) was: 1,046 (3,266) for “opto stim” and 717 (2,689) for “opto stim + obj”. For (M) the number of runs was 1,189 for “opto stim” and 764 for “opto stim + obj”.

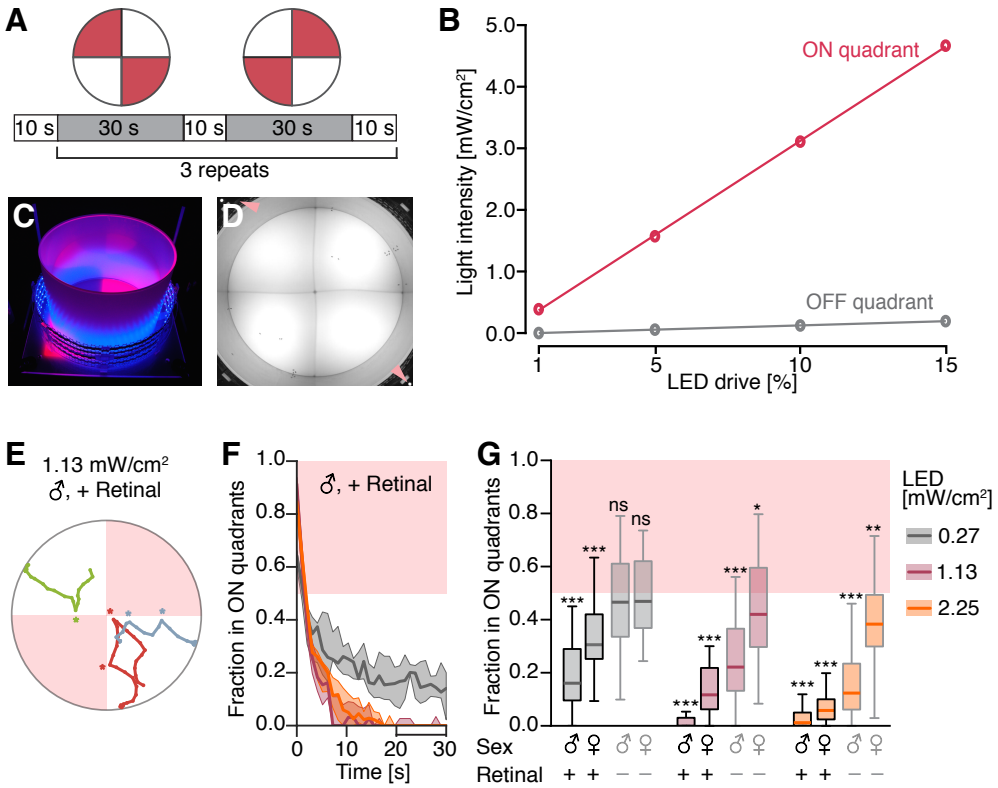

Figure S5: Calibration of *"virtual heat"* stimulus in freely walking flies, Related to Figure 5.
(**A**) Schematic of the quadrant assay trial structure. (**B**) Photograph showing the lighting conditions during the quadrant assay. Blue LEDs around the arena wall provide ambient light visible to flies. The red light illuminating two quadrants is invisible to flies. (**C**) One frame from a video recorded during a trial with male HC-GAL4 x 10xUAS-ChrimsonR flies. Two IR lights at the corners of the image (arrowheads) indicate which quadrants are illuminated. (**D**) Measured light intensities as a function of % LED driver current in the illuminated "ON" (red points) and the not illuminated "OFF" quadrants (grey points). Measurements were performed during continuous light illumination with a power meter (see Methods). The solid lines are the linear regressions for the five measurements. ON quadrants: $y = 0.30x + 0.08$, $R^2 = 1.00$. OFF quadrants: $y = 0.01x - 0.00$, $R^2 = 1.00$. (**E**) Short fragments of walking traces from three male HC-GAL4 > ChrimsonR flies in the free walking quadrant assay (fly identity color-coded). Asterisks mark turns away from the illuminated quadrants (red-shaded regions). (**F**) Fraction of male HC-GAL4 > ChrimsonR flies residing in the illuminated quadrants over the course of the 30 s long stimulation block. The median (line) and IQR (shaded region) are shown for three experimental groups with different stimulation light intensities (see legend in (G)). Values below 0.5 indicate avoidance of the optogenetic stimulus. (**G**) Comparison of different stimulation protocols in the quadrant assay. For each group the average fraction of flies in the illuminated quadrants measured in the last 10 s of the stimulation repeat (bar in time axis in F) is shown. Statistical significance levels refer to difference from 0.5 (two-sided one-sample t-test, see Methods for details). Significance codes: "ns" $p > 0.1$, "*" $p \leq 0.05$, "**" $p \leq 0.01$, "***" $p \leq 0.001$.

Aversive conditioning with HC activation as reinforcement

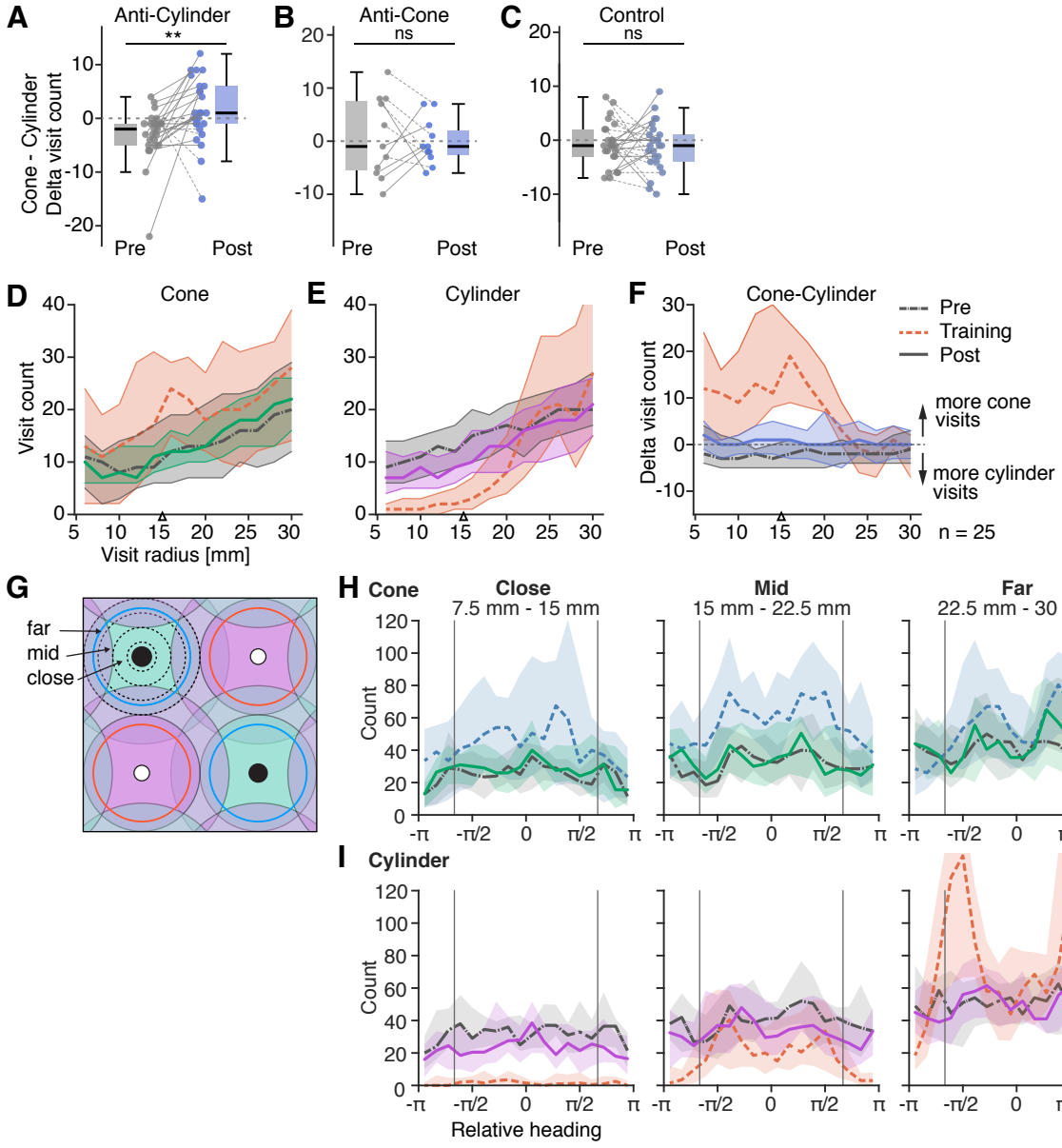

Appetitive conditioning attempt using Gr64a activation as reinforcement

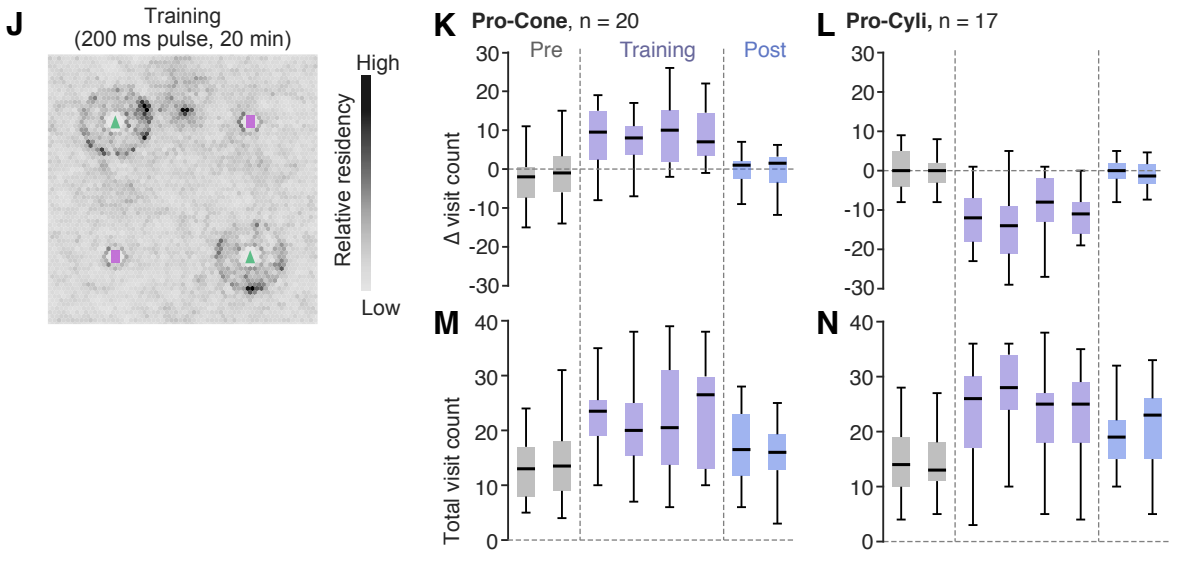

Figure S6: Extended data on object shape conditioning, Related to Figure 6.
(**A**-**C**) Delta visit count in the pre- and post-trial for the three conditioning protocols presented in Figure 6 (F-H). Lines connect data points from the same fly (solid line: increased cylinder preference; dashed line: no change or decreased cylinder preference). Positive values correspond to a relative preference for visiting cones. For each group, we performed a paired t-test with for alternative hypothesis that the true location shift is 0. Anti-cylinder training (A): n=22, p=0.00305 (**), anti-cone training (B): n=11, p=0.74895 (ns), control training (C): n=22, p=0.56107 (ns). (**D, E**) Visit counts for cone (D) and cylinder (E) as a function of visit radius. Median (thick line) and IQR (shaded region) are shown for the three trials. Line style of the median encodes trial identity (see legend in C, right). (**F**) Delta visit count (cone visits – cylinder visits) as a function of visit radius. Visualization as in (D, E). (**G**) Schematic illustrating visibility of cones and cylinders within the square unit tile of the *cone and cylinder forest*. Size of virtual heat and cool zones are marked around cones (dark circles) and cylinders (white circles). Shading marks visibility of cones (green) and cylinders (magenta, see Figure S1I for additional explanation). Black dashed circles mark distance ranges analyzed in (H, I). (**H**, **I**) Relative heading distributions in pre-, train- and post-trials for different distances from the reference object (H: cone; I: cylinder). Median (line) and IQR (shaded region) shown for heading distributions computed for each fly (only flies with minimum number of 5 visits to any object were considered, n=22). Grey vertical lines mark edges of the panoramic screen within the visual field of view. (**J-N**) Attempted appetitive conditioning based on Gr64f-Gal4 neuron activation in the *cone and cylinder forest* VR environment. (**J**) Residency distribution visualized as in Figure 3E for the training trial (20 min, stimulation around cones at 20 mm radius). (**K, L**) Comparison of shift in shape preference across two experimental groups: pro-cone training (K) and pro-cylinder training (L). (**M, N**) Total visit counts for pro-cone training (M) and pro-cylinder training (N). Sample sizes after selection are noted in the figure. Shape preference (number of cone visits minus the number of cylinder visits) and total visit count (number of cone visits plus the number of cylinder visits) was quantified for each fly in intervals of 5 min. Data from all flies that made at least 5 visits to any object in each trial is presented as boxplots (black line: median, box spans the 25^{th} to the 75^{th} quartile). Significance codes: “ns” $p > 0.1$, “*” $p \leq 0.05$, “**” $p \leq 0.01$, “***” $p \leq 0.001$.